Research Square

Preprints are preliminary reports that have not undergone peer review.
They should not be considered conclusive, used to inform clinical practice,
or referenced by the media as validated information.

Wide range tunable photonic frequency synthesiser with low and non-scaling phase noise

Zhixin Liu

zhixin.liu@ucl.ac.uk

University College London https://orcid.org/0000-0002-9681-7933

Amany Kassem

University College London

Zichuan Zhou

University College London

Alex Bennett

University College London

Izzat Darwazeh

University College London

Article

Keywords:

Posted Date: March 23rd, 2026

DOI: https://doi.org/10.21203/rs.3.rs-8888348/v1

License: This work is licensed under a Creative Commons Attribution 4.0 International License.
Read Full License

Additional Declarations: Yes there is potential Competing Interest. A.K. and Z.L. are inventors on patent application No. PCT/EP2025/057707 related to the subject matter of this work.

Wide-range tuneable photonic frequency synthesiser with low and non-scaling phase noise

Amany Kassem[1], Zichuan Zhou[1], Alex Bennett[1], Izzat Darwazeh[1], and Zhixin Liu[1] ✉

[1]Department of Electronic & Electrical Engineering, University College London, London, UK

Abstract

Frequency synthesis is central to communications, sensing, navigation and spectroscopy, requiring low phase noise and wide frequency tunability across the microwave to millimetre-wave bands. However, conventional electronic frequency synthesis suffers from phase noise that scales quadratically with output frequency and from intrinsically limited tuning bandwidth, leading to bulky, power-hungry architectures at high frequencies. Many photonic approaches achieve low phase noise with ultra-stable lasers and optical frequency combs, but typically lack wide tunability and impose size, weight and power constraints. Here, we demonstrate a photonic frequency synthesiser based on an optical harmonic locking that overcomes these limitations by locking widely spaced narrow-linewidth lasers using only low-frequency, low-bandwidth electronics. The approach enables continuous, referenced frequency generation with Hz-level resolution from 0.375 to 170 GHz, while exhibiting non-scaling phase noise over offset frequencies from 200 kHz to 10 MHz. We record a phase noise of -146 dBrad^2/Hz at 10 MHz offset, and a fractional frequency instability of $3{\times}10^{-13}$ at 1 s, resulting in a reduction of timing jitter with increasing carrier frequency 12 fs at 170 GHz, outperforming state-of-the-art commercial signal generators. We further demonstrate 1024-QAM transmission at a 150 GHz carrier, highlighting the potential of photonic synthesis for next-generation high-frequency communication and sensing systems. The architecture is compatible with integrated photonic implementations, promising potential chip-scale deployment.

1 Introduction

A frequency synthesiser generates a sinusoidal signal that can be modulated, transmitted and processed, necessitated by numerous applications including communications, sensing, ranging, to timing, navigation and spectroscopy [1, 2, 3, 4]. These various applications require generating signals with precise frequency and low phase noise spanning from 10s of MHz to 100s of GHz.

For example, radar systems use 2-18 GHz microwave for earth observation [5] and millimetre (mm) wave up to 240 GHz for environmental monitoring [6, 7]. In such systems, low phase noise signal sources are essential to achieving high detection probability and imaging quality. In atomic clocks and spectroscopy, precise and low phase noise signals are essential to enable accurate probing of narrow atomic absorption lines, such as the 9.192-GHz hyperfine ground-state transmission in Caesium clock and the >100GHz absorption lines in atmospheric gas detection [8]. In mobile and satellite communications, transceivers modulate amplitude and phase of signals in sub-6GHz frequency region for broader coverage, while employing >60 GHz frequencies for high capacity data transmission, in territorial links and space, which require precise and low phase noise signals to maximize capacity and spectral efficiency [9, 10].

An ideal frequency synthesiser should be capable of generating any required frequency with low phase noise, while also offering a compact footprint, low cost and low power consumption [11, 12]. However, conventional electronic frequency synthesis approaches, such as electronic phase locked loops or frequency multiplier-based methods, inherently suffer from phase noise that increases quadratically with the output frequency [13]. Typically, the power spectrum density (PSD) of phase noise scales with $(f_s/f_{ref})^2$, where f_s is the synthesised frequency and f_{ref} is the reference frequency. As a result, systems operating at high frequencies, particularly in the millimetre-wave band (30-300 GHz), experience substantial performance degradation [9, 14].

Furthermore, the frequency tuning range of a single synthesiser is inherently constrained by the bandwidth of its oscillator and multipliers. Achieving broadband electronic frequency synthesis therefore requires a complex signal chain comprising multiple synthesisers, each typically covering only a 10-20 GHz span, with their outputs routed to a common port through frequency-selective switches to enable continuous tuning over ranges approaching 70 GHz [15]. This architectural complexity results in bulky, expensive, and power-hungry signal generators, thereby restricting their application primarily to laboratory and industrial test equipment.

Photonics-based approaches offer unique advantages over conventional all-electronic techniques, particularly in the >70GHz regime, where electronics face fundamental limitations. Over the past decade, rapid progress in narrow-linewidth lasers [16, 17, 18] , broadband photodetectors (PDs) [19, 20, 21] , optical frequency combs, and associated frequency division, multiplication, and locking techniques has enabled synthesis of radio frequency (RF) signals with low noise and high spectral purity [3, 22]. With continued advances in photonic integration, such systems have the potential to achieve substantially reduced size, weight, and power consumption (SWaP), paving the way for compact and efficient high-frequency signal generation. For example, optical frequency division technique transfers the stability of an ultra-stable optical cavity to the RF domain by detecting a frequency comb locked to optical reference [1, 2, 23, 24, 25]. This method significantly reduces phase noise at low frequency offset regime, typically from 1 mHz to about 10 kHz. However, the phase noise at higher offset frequencies (e.g. >100KHz) remains high as it is dominated by the output stage of electronic synthesiser, which also limits demonstrations in the microwave frequency region and to tuning range of a few GHz [2]. The direct photomixing method generates an RF signal by beating the outputs of two lasers on a PD, with stabilisation by an optical phase-locked loop (OPLL) [26, 27]. Nevertheless, conventional OPLLs require a broadband electronic local oscillator (LO), a high-speed PD, and RF mixers capable of operating at frequencies comparable to the lasers' spacing. As a result, it encounters similar challenges to conventional electronic frequency synthesisers, including phase noise scaling, limited tuning range and high cost.

Our work addresses the above-mentioned challenges by proposing and optimally implementing an optical harmonic lock loop (OHLL) in conjunction with state-of-the-art narrow-linewidth lasers. This approach enables locking widely frequency-spaced lasers with substantially reduced phase noise using only low frequency and low bandwidth electronic components, enabling the generation of stable, referenced and continuously tuneable frequencies with Hz-level resolution across the entire 0.375–70 GHz range.

Specifically, we demonstrate low and non-scaling phase noise in the 200 kHz–20 MHz frequency offset region, thereby overcoming the quadratic scaling limit inherent to the conventional electronic approaches. As a result, the jitter (integrated over 10 Hz−10 MHz) reduces as the generated frequency increases, contrary to conventional electronic synthesisers which typically have a fixed jitter due to quadratic scaling of phase noise. Following this principle, we demonstrate an integrated jitter of 12 fs at 170 GHz, outperforming the state-of-the-art commercial signal generator. Based on our photonic signal generator, we investigate the impact of phase noise on a D-band millimetre-wave communication system and demonstrate up to 1024 QAM modulation, showing that low phase noise is essential to achieving high signal to noise ratio (SNR) and high spectral efficiency for communications in the mm-wave bands.

Rooted in classic optical heterodyne beating, our tuneable photonic synthesiser begins with a combination of two low-linewidth continuous wave (CW) lasers, whose frequency separation can be tuned over 5−170 GHz range by adjusting the wavelength of each laser. The combined CWs beat at the PD, generating an RF signal at a frequency f_c, where $f_c = f_1 - f_2$, equals the frequency separation between the two lasers. The phase noise of the resulting beat signal is a combination of the phase noise of the individual laser, plus the shot and thermal noise from the PD. To minimise the impact of thermal and shot noise, the lasers are operated at their highest power (about 25 mW), and consequently, the phase noise of the RF signal is governed by the intrinsic phase noise of the lasers.

To study the impact of laser phase noise on the generated RF signals, we employed three lasers forming two pairs: Pair 1 consists of a 40-Hz-linewidth whispering gallery mode laser and a 600-Hz-linewidth fibre laser, while Pair 2 comprises the same 40-Hz-linewidth laser combined with a 7-Hz-linewidth whispering gallery mode lasers (see supplementary 1 for the laser noise characterisations).

The key challenge we address here is to phase-lock two widely separated CW lasers, such that the generated RF signal can be tuneable, low phase noise and frequency-referenced. This is achieved using our optical harmonic lock loop (OHLL), which relates the phase and frequency of the CWs by simultaneously expanding the combined signals using the same harmonic generator, as shown in Fig.1a. Here, we used a phase modulator (PMod) driven with an RF synthesiser operating within 5-30 GHz (f_m) as the harmonic generator. By driving the PMod with sufficient RF power, we generate high order harmonic tones following the Jacobi-Anger expansion [28]. yielding two comb-like signals in the optical domain (Fig.1a).The upper sideband (USB) tones of laser 1 expansion and the lower sideband (LSB) tones of

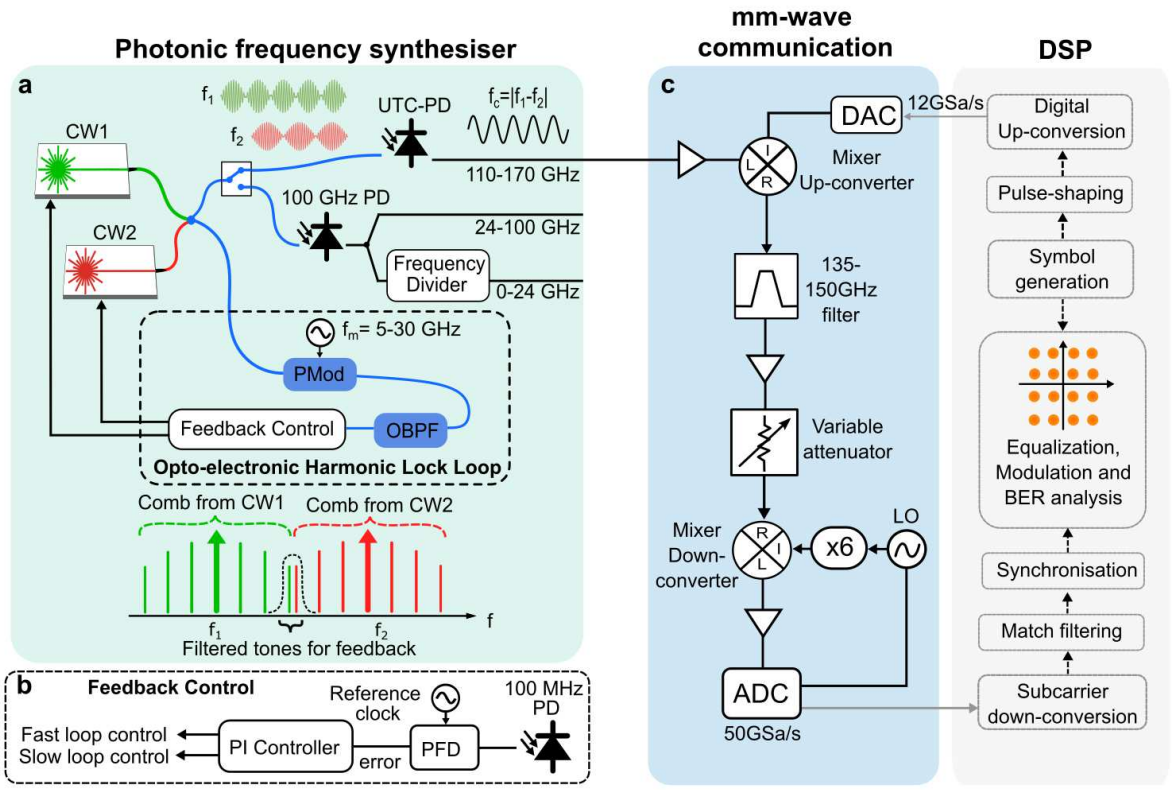


Figure 1: (a) Operational principle of our proposed photonic frequency synthesiser. and (b) the electronic feedback (c) the mm-wave synthesiser enabled communication system.

laser 2 expansion overlap in the centre of the spectrum and are subsequently filtered out using an optical bandpass filter (OBPF) of about 10 GHz bandwidth, leaving only the nth USB tone from comb 1 and the nth LSB tone from comb 2.

By tuning f_m, we can control the frequency separation of the filtered harmonic tones to sub-100 MHz, such that the filtered tones can be detected by a low bandwidth (e.g. <100 MHz) PD but with high impedance load, which permits high gain with reduced thermal noise. Additionally, the modulator-induced phase noise in the upper and low side bands is conjugated-symmetric, resulting in a cancellation of the in-phase noise component. This scheme effectively maps the phase and frequency difference between two widely separated CWs to sub-100-MHz intermediate frequency (IF) signal, enabling feedback control with low added noise. The IF signal is subsequently fed to a phase frequency detector (PFD), where it is compared to a 25 MHz local oscillator (LO) to produce a phase error signal. This error signal feeds a proportional integral (PI) controller that controls the frequencies of the CW lasers using fast and slow loop control as shown by Fig.1b. Both f_m and the 25 MHz LO are locked to the same 10 MHz quartz oscillator, allowing generation of frequency-referenced RF signals.

A 100-GHz bandwidth PD was used to generate RF signals up to 105 GHz, where the mm-wave signals above 24 GHz are directly generated from the PD output. The sub-24 GHz signals are generated by passing the PD output through a 55-GHz programmable divider. The 110-170 GHz signals are generated by switching the optical port into a uni-travelling-carrier (UTC) PD. Details are described in Methods.

Fig.1c shows the proof-of-concept experiment using our photonic frequency synthesiser as transmitter LO for mm-wave communications. We generate a 153-GHz mm-wave signal from the UTC-PD using laser Pair 2. The output of the UTC-PD was amplified to 6 dBm for optimal operation of a D-band (110-170 GHz) balanced mixer as LO. The communication signal is a 1-GBaud signal-carrier quadrature amplitude modulation (QAM) signal, which is upconverted to 153 GHz using the D-band mixer, and is subsequently filtered with a 135-150 GHz filter to create a single-side band (SSB) signal. The SSB signal is downconverted to sub-10 GHz before being digitized by a 50 GSa/s ADC for digital signal processing (DSP). A variable RF attenuator is used to emulate link loss to study receiver sensitivity.

2 Results

Low-noise signal generation

We first characterise the phase noise and jitter performance of our photonic synthesised frequencies, as shown in Fig.1a.The jitter is calculated by integrating the measured phase noise over 10 Hz − 10 MHz using equation 1,

$$\sigma = \frac{1}{2\pi f_c}\sqrt{2\int_{10}^{10M} \mathscr{L}(x)\, df} \tag{1}$$

where $L(f)$ is the SSB phase noise, f_c is the carrier frequency.

The results are compared with the conventional 'LO + multiplier' approach using three representative all-electronic synthesisers as LOs: a module synthesiser (SignalCore SC5511) and two instrument synthesisers (Rohde & Schwarz SMA100B with ultra-low phase noise option and the standard Rohde & Schwarz SMA100B). Detailed noise characterisationis shown in supplementary 2.

Due to the quadratic scaling of phase noise with carrier frequency, conventional electronic synthesisers exhibit constant jitter across the entire frequency range. In contrast, the photonic synthesised signals exhibit frequency independent phase noise, resulting in jitter that is inversely proportional to the carrier frequency, f_c. By employing OHLL with ultra-low noise lasers (laser pair 2), the photonic frequency synthesiser consistently outperforms the module synthesiser, which has a fixed jitter of 247 fs, across the full frequency range. Compared to the standard instrument synthesiser, which exhibits approximately 42 fs jitter, our photonic frequency synthesiser achieves lower jitter across the entire measured frequency range (Fig. 1a). In contrast to conventional electronic synthesisers, the jitter decreases as the generated frequency increases, reaching approximately 12 fs at 170 GHz. We do not yet surpass the instrument synthesiser equipped with the ultra-low phase noise option from Rohde & Schwarz, which achieves approximately 8 fs jitter, although the performance gap narrows at higher frequencies. Although our measurements are currently limited to 170 GHz due to equipment availability, laser pair 2 can be tuned and locked at frequency separations up to 300 GHz while maintaining the same optical phase-noise performance. This suggests a projected integrated jitter of approximately 7 fs at 300 GHz.

Although superior performance is achieved in the high frequency region, the constant phase noise leads to increased jitter in the low frequency region. To achieve high performance across the entire 0.375 − 170 GHz range, we employ a frequency divider for sub-24GHz signal generation. This leads to a constant jitter of approximately 38 fs over 3-24GHz. Limited by the thermal noise of the frequency divider, the jitter of the sub-3 GHz signal increases towards lower frequencies and exceeds that of the standard instrument synthesiser at 0.375 GHz.

We also experimentally demonstrate the impact of laser phase noise on synthesised RF signals by comparing the jitter of laser pair 2 (red square) with laser pair 1 (blue circle). Approximately 2.5 times reduction of jitter is achieved by replacing the 600-Hz-linewidth fibre laser with a 7-Hz-linewidth whispering gallery mode laser.

A comparison of their-yielded RF phase noises at 170GHz is plotted in Fig.1b, where the dashed lines show performance of the free-running lasers. Similar to previous demonstration [29], the flicker noise and random walk in free-running lasers led to significantly increased noise in the low frequency offset region (100-100 kHz). Our OHLL significantly reduces this with a locking bandwidth of approximately 100kHz, demonstrating more than 50 dB noise suppression in the sub-1kHz region for both laser pairs. The locking bandwidth is limited by the loop delay, which is approximately 50 ns due to the fibre pigtails. Further improvement is possible with photonic integrated circuit, as discussed later. For both laser pairs, the high frequency phase noise in the >1MHz region exhibits similar performance, with the noise floor governed by shot noise and a resonance peak near 3.5 MHz due to the loop response. The improvement of phase noise mainly comes from the 100 Hz−1 MHz region, in which the whispering gallery mode laser outperforms the fibre laser.

Fig. 1c shows the phase noise of pair 2 laser generated signals from 10 GHz to 170 GHz. Phase noise in the high frequency region (>20 kHz) offset remains consistent regardless of the generated frequency. In contrast, phase noise in the low frequency (100 Hz to 1 kHz) offset region increases with the carrier frequency. This is due to the RF noise from the electronic synthesiser driving the phase modulator, which is coupled into the OHLL. Between 1kHz and 20kHz, the phase noise curves slowly converge. Although one can see clear phase noise difference in the low frequency region, the integrated jitter is dominated by the >10 KHz noise, and consequently, reduced jitter shown in Fig. 2a.

Fig. 1d shows the phase noise of the divided frequencies with an input at 48 GHz. The phase noise reduces quadratically following the frequency multiplication/division rule, resulting in similar jitter

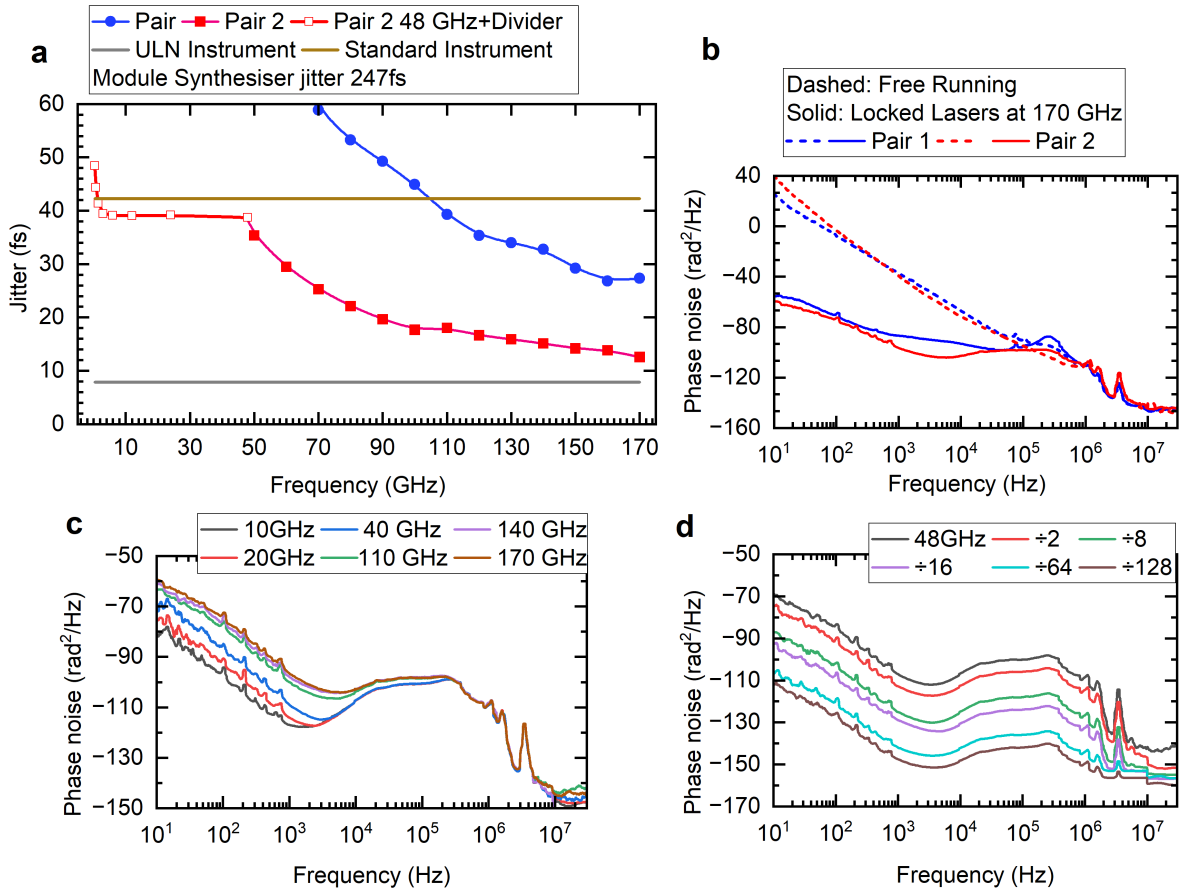


Figure 2: Phase noise performance of synthesised frequencies from 0.375 GHz to 170 GHz.(a) Comparison of integrated jitter (10 Hz−10 MHz) measured from our photonic frequency synthesiser using laser pair 1 (blue circle) and laser pair 2 (red square), state-of-the-art electronic module synthesiser (not shown in the figure) but has fixed jitter of 247 fs, standard instrument synthesiser (brown line) and ultra-low noise instrument synthesiser (grey line). Solid curves interpolate the measured results using spline fitting. The open square marker shows the jitter of the divided frequencies in the 0.375 GHz−24 GHz region, where the PFS outputs 48 GHz. The module synthesiser (triangle markers) represents a typical synthesiser performance in applications such as microwave communications, radar, and microwave digital-to-analog converter (DAC) and analog to digital converters (ADC). The instrument synthesiser (marker or line) represents the current state-of-the-art performance in electronic synthesisers employed in research, science and industrial qualifications. (b) Phase noise of photonic synthesised frequencies at 170 GHz using free running lasers (dashed lines) and our OHLL (solid lines). Blue and red curves show results using laser pair 1 and pair 2, respectively. (c) Phase noise of photonic synthesised frequencies over 10 GHz−170 GHz. The signals are directly generated from PDs (without involving divider) using Pair 2. The 110−170 GHz signals are generated from the UTC-PD and the 10 GHz−40 GHz signals are generated from the 100-GHz PD. (d) Phase noise of 0.375 GHz−24 GHz signals generated from the RF divider, where the divider input is a 48 GHz is directly generated from PD using OHLL. By dividing the frequencies, we obtained reduced phase noise that enables maintained low integrated jitter in Fig.2a in the 3−24 GHz region. The increase of the jitter in the sub-3GHz is due to the constant thermal noise floor in the >1MHz offset region.

between 3–24 GHz, as shown in Fig. 1a. However, the sub-3 GHz outputs show reduced gain, particularly in the >1 MHz offset region, due to the thermal noise limit, leading to increased jitter.

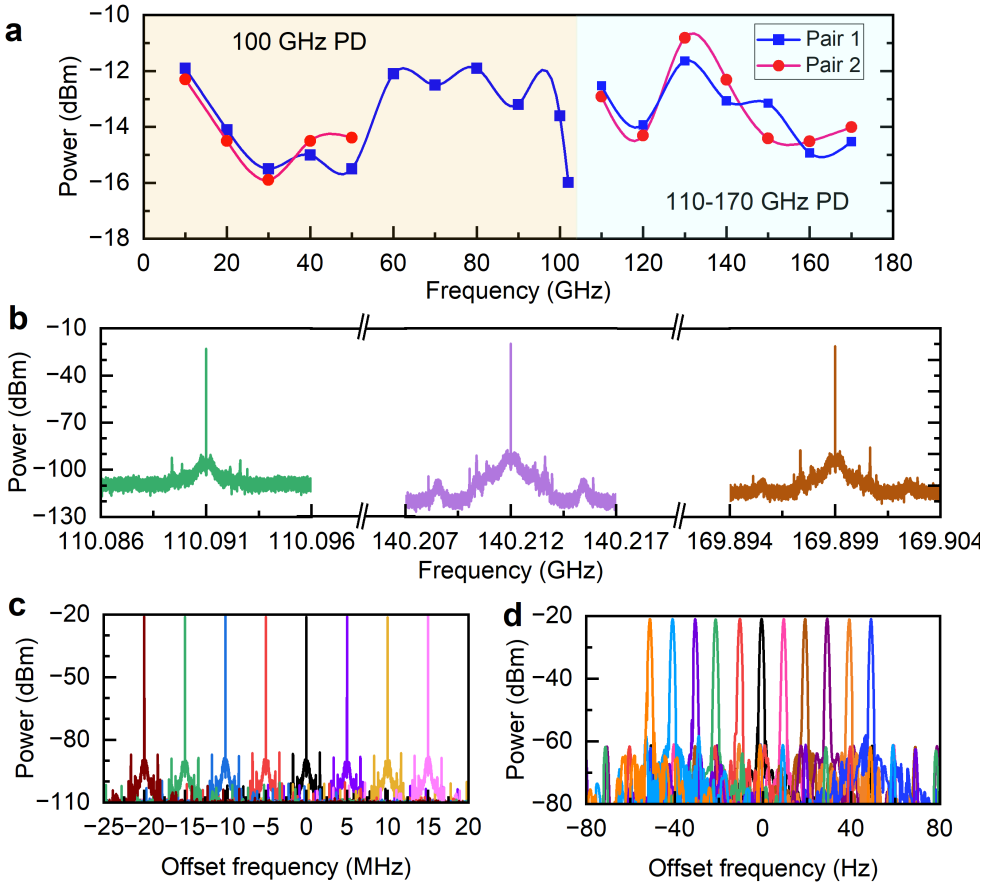


Figure 3: Tunability of our photonic frequency synthesiser. (a) Measured RF power of directly synthesised frequencies using both laser pair 1 (blue square markers) and laser pair 2 (red circle markers). The sub-102 GHz results are generated using the 100 GHz PD, while the 110–170 GHz results are generated using a D-band UTC-PD. The 50–100 GHz range for laser pair 2 is not available due to limitations in the measurement instruments during the experiment. (b) RF spectra of the synthesised signals at 110 GHz (green), 140 GHz (purple) and 170 GHz (brown), respectively. (c) RF spectra of synthesised frequency tuning at 5 MHz interval when centred at 170 GHz, measured with a resolution of 100 Hz. Spectra at different frequency offsets are plot in the same figure using different colours. (d) Ultra-fine frequency tuning at 10 Hz interval with a resolution of 1 Hz. Spectra at different frequency offsets are plot in the same figure using different colours.

Frequency tuneability

Fig. 3a shows the RF signal power measured across 5-170 GHz using both laser pair 1 (blue circle) and pair 2 (red quare). In the 5-102 GHz region, the RF power varies by approximately 4 dB due to combined frequency responsivities of the PD and RF components. The roll-off at 100 GHz is due to the bandwidth limitations of the 100 GHz PD. In the 110-170 GHz range, the power variation of the RF signals is approximately 3 dB, with a peak occurring at around 130 GHz, corresponding to the responsivity of the employed UTC-PD. The slight discrepancy between pair 1 and pair 2 is due to the use of different measurement tools and their calibrations (see Method).

Fig. 3b shows the measured RF spectra of the photonic synthesised frequencies at 110, 140 and 170 GHz, generated using laser pair 2. The synthesised signals exhibit a spurious free dynamic range (SFDR) of approximately 55 dB, limited by the side modes of the lasers.

Fig. 3c demonstrates the fine-tuning capability of our photonic synthesiser, displaying the measured spectra of 170-GHz-centred signals with 5 MHz frequency intervals. An ultra-fine tuning of 10 Hz interval is demonstrated in Fig. 3d. The fine tuning is achieved by adjusting the LO frequency of the phase frequency detector (PFD), enabling a frequency tuning up to 35 MHz, limited by the PFD's bandwidth.

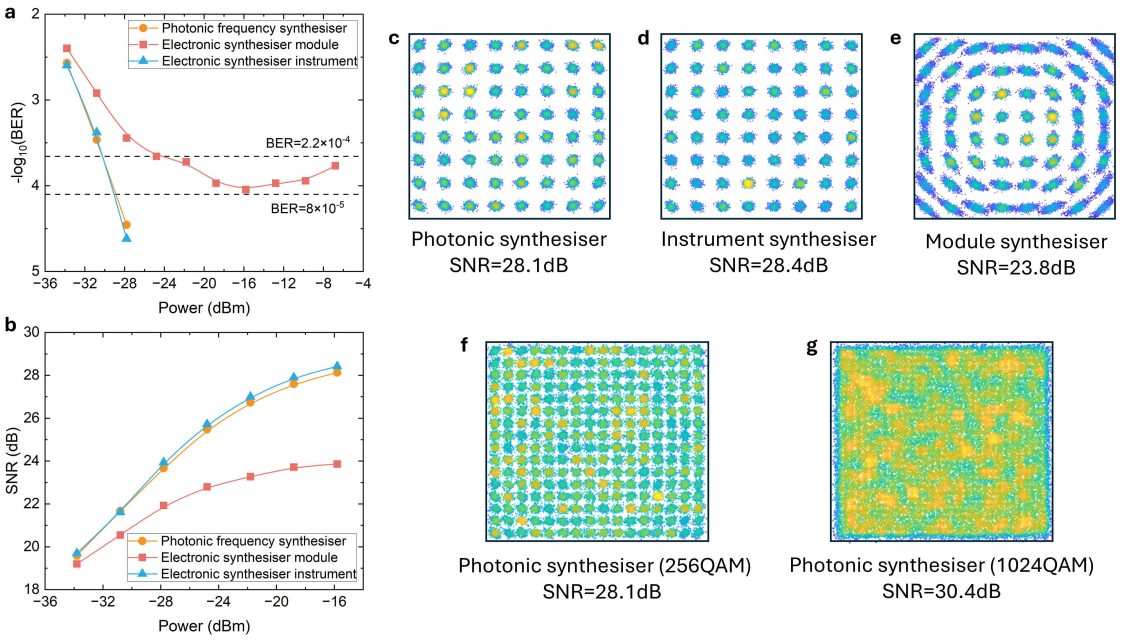


Figure 4: Impact of LO phase noise on mm-wave communication systems centred at 153 GHz. (a) BER versus received RF power for different transmitter local oscillators (LOs): an electronic synthesiser module (red squares), an electronic synthesiser instrument (blue triangles), and the proposed photonic frequency synthesiser (orange circles). (b) SNR of 64 QAM signalling versus received RF power for different transmitter local oscillators (LOs): an electronic synthesiser module (red squares), an electronic synthesiser instrument (blue triangles), and the proposed photonic frequency synthesiser (orange circles). (c)-(e), constellation diagrams of 64 QAM using different Los measured at a received power of -16 dBm: (c) our photonic frequency synthesiser, (d) electronic instrument synthesiser (d), electronic module synthesiser (e) f-g, constellation diagrams using our photonic frequency synthesiser as LO: (f) 256 QAM; (g) 1024 QAM.

The PFD supports ultra-fine tuning with Hz-level precision, referenced to the 10 MHz reference oscillator. The demonstration is limited to 10 Hz due to the resolution limit of the spectrum analyser. In principle, sub-Hz precision tuning is possible with a stable reference oscillator.

mm-wave communications

We compare the performance of our photonic frequency synthesiser with all-electronic synthesisers used as transmitter LOs in the mm-wave communication system. Both all-electronic synthesisers operate at 19.125 GHz and are frequency-multiplied to 153 GHz using a ×8 multiplier (details in supplementary 3). All LOs operate at 10 dBm for optimal mixer operation.

Fig. 4a shows the measured BER versus received power at the input of the receiver mixer for 1-GBd 64-QAM signals, corresponding to a data rate of 6 Gb/s. The corresponding SNR is plotted in Fig. 4b. Our photonic frequency synthesiser and the ultra-low noise instrument synthesiser show comparable performance, while the module synthesiser results in approximately 4 dB power penalty at the hard-decision BER threshold (KP4-FEC, BER = 2.2×10^{-4} [30]) with a BER floor of 1×10^{-4}. This penalty results from phase noise, where the symbol clusters show rotation due to the relatively high phase noise of the module synthesiser.

The SNR of both the photonic and ultra-low noise instrument synthesisers increases linearly with received power up to −22 dBm, beyond which further improvement is limited by saturation in the receiver mixer. By contrast, the module synthesiser exhibits only marginal SNR enhancement with increasing received power, reaching a maximum SNR of approximately 23 dB at −16 dBm.

The low phase noise of the photonic synthesiser enables high-order modulation formats, supporting 256-QAM and 1024-QAM and yielding capacity gains of 33% and 67%, respectively, relative to the module synthesiser, which is limited to 64-QAM. At lower received powers, the SNR and BER of all

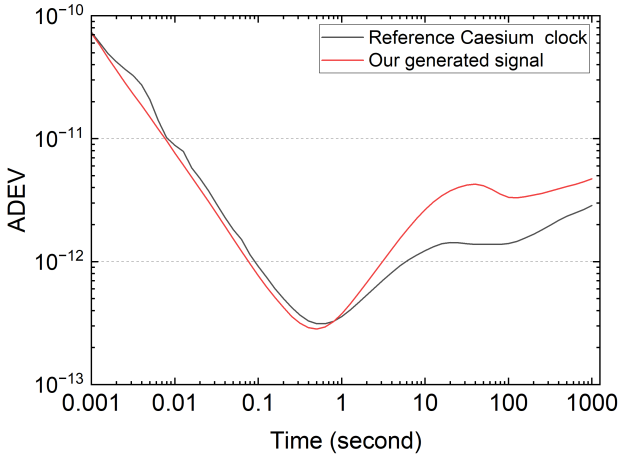


Figure 5: Stability characteristics of photonic frequency synthesiser with a 10 MHz Caesium clock as reference. The red curve shows the ADEV of the synthesised 48 GHz signal, while the black curve shows the ADEV of the Caesium reference itself.

three synthesisers converge as the receiver thermal noise becomes the dominant performance constraint.

3 Discussion

We demonstrate technique that enables precise, referenced, and continuous tuning of laser-based frequency synthesis over an ultra-wide range of 0.375–170 GHz. To the best of our knowledge, this represents the widest tuning range demonstrated by a single synthesiser system. This capability is achieved by exploiting the advantages of the OHLL, including its partial noise cancellation and the use of a high-impedance optical receiver to generate a high-SNR error signal, permitting accurate capturing of the frequency and phase difference between the laser pair. Second, we demonstrate low phase noise RF signal generation in the mm-wave regime that outperforms state-of-the-art commercial electronic synthesisers. The proposed photonic frequency synthesis approach overcomes the phase noise scaling limitations inherent to conventional electronic techniques, offering a promising pathway towards next-generation high-frequency synthesisers. Finally, we show that low phase noise signal generation is critical for achieving high capacity mm-wave communications. Experimental results demonstrate that the proposed photonic frequency synthesiser enables high spectral efficiency data transmission, validating its potential for future broadband wireless systems.

The OHLL-based photonic frequency synthesiser offers several distinct advantages over existing techniques. For example, conventional heterodyne based OPLLs [26, 27] typically require an LO operating at a frequency comparable to that of the generated RF signal to down-convert it to an IF for feedback control. This significantly increases system cost and power consumption due to the need for broadband RF components, including wideband mixers, RF amplifiers, high speed PDs and high frequency LOs.

Locking lasers to frequency combs or optical cavities can enable high performance signal generation in the Terahertz regime [4, 6]. However, it requires additional cavities or comb sources, and the frequency tunability (range and resolution) is limited due to the fixed comb spacing and free spectral range. Different from frequency comb and optical cavity-based locking, OHLL only locks the relative phase and frequency between the lasers. This enables the system to be optimised specifically for linking the phase and frequency of two individual lasers, rather than providing an absolute optical frequency reference, as required in techniques such as optical injection locking (OIL) or direct comb locking [31, 32, 33].

Fig. 5 shows the fractional instability of the direct synthesised 48-GHz signal, presented as Allan deviation (ADEV), when using a 10 MHz Caesium clock as the reference oscillator. For comparison, the ADEV of the 10 MHz caesium reference itself is shown as the black curve. A high stability of 3×10^{-13} at a 1s averaging time is achieved. Compared to the Caesium clock, the synthesised 48 GHz signal exhibits slightly reduced stability for averaging times above than 1s, with ADEV increased from 2.8×10^{-12} to 4.5×10^{-12} at 1000s averaging time, which is likely due to the added noise in the feedback system.

Recent hybrid and heterogeneous photonic integration have enabled ultra-low noise lasers with 10s of milliwatts of optical power, providing similar power and noise performance as the discrete lasers used in

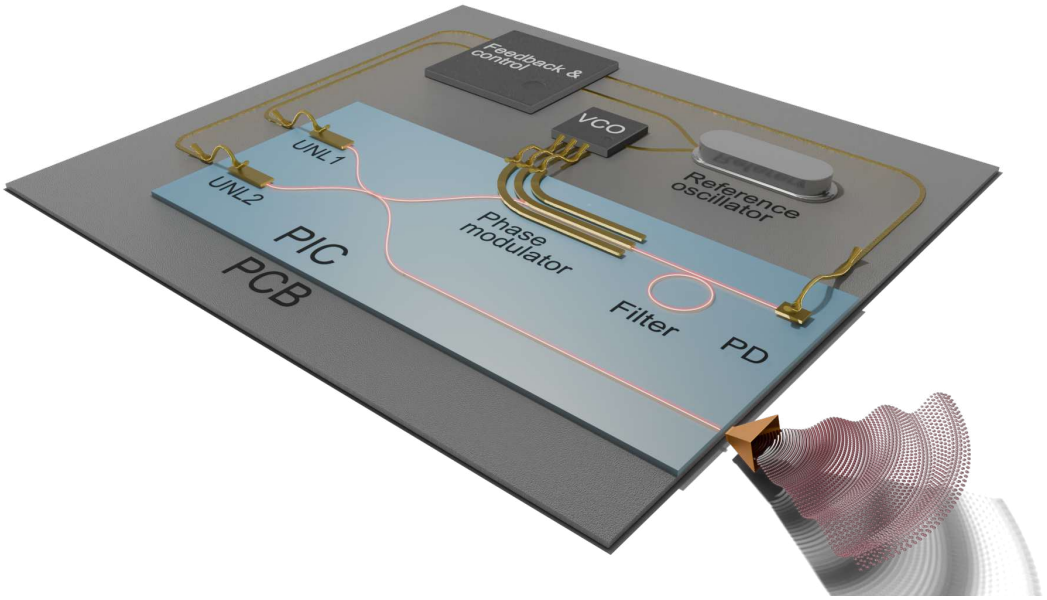


Figure 6: Envisaged schematic of an integrated photonic circuit based synthesiser. The integrated system incorporates the same key photonic elements used in this work. Two low linewidth lasers are combined using a 2×2 multi-mode interferometer (MMI), with the upper branch output port phase modulated by the output of a voltage-controlled oscillator to generate comb tones, and the lower branch port connect to a PD for output. The closely spaced harmonic tones are filtered by an optical cavity filtered before detected by a PD for generation error signal. Electronic printed circuit board that drives the PIC, including a reference oscillator, a voltage-controlled oscillator and a feedback unit containing PFD and PI controller.

this proof-of-concept demonstration. For example, ultra-low loss silicon nitride (SiN) extended cavities, pumped with indium phosphide (InP) gain sections, have been realised through butt-coupling [17] and heterogeneous integration approaches [18]. Fundamental linewidths <40Hz have been demonstrated with SiN using both hybrid [17] and heterogeneous integration [18]. Additionally, on thin film lithium niobate (TFLN), researchers also demonstrated a 550-Hz lasers with potential for further linewidth reduction [34]. Laser integration with modulators, filter, and detectors has also been previously demonstrated on such platforms, which can be utilised for full integration of all the optical components comprising the locking system. Photonic integration can greatly reduce loop delay, improving on the locking bandwidth that could lead to further improved RF noise performance [35].

4 Methods

Optical harmonic locked loop

The system was demonstrated using two laser pairs with distinct linewidths to examine how linewidth affects overall performance. Pair 1 combined a 600-Hz-linewidth fibre laser with a 40-Hz-linewidth whispering-gallery-mode (WGM) laser. The fibre laser (NP Photonics, the Rock) has a frequency modulation (FM) bandwidth of about 1 kHz. The 40-Hz WGM laser (OEwaves, Hi-Q C-band laser) has a FM bandwidth near 100 kHz. Pair 2 combined the same 40 Hz WGM laser with a 7-Hz WGM laser from the same manufacturer. Each pair was evaluated independently, using the same optical/RF hardware configuration.

The optical outputs of the lasers were combined using a 50/50 polarisation-maintaining (PM) coupler, producing two identical combined outputs. One of these outputs was routed to the RF signal generation branch. A photodiode with a bandwidth of 100 GHz and a responsivity of approximately 0.5 A/W was used to generate signals up to 102 GHz. For mm-wave generation in the 110–170 GHz range, a uni-travelling-carrier (UTC) photodiode (NTT IOD-PMD-14001) was employed. For output frequencies below 24 GHz, a directly synthesised 48 GHz signal was divided using a programmable frequency divider

with configurable division ratios from 2 to 128. This approach enabled the generation of tuneable, low-phase-noise microwave outputs without modifying the optical setup.

The second combined output was used to generate error signals for stabilising the frequency and phase difference between the two lasers. The combined optical signal was phase-modulated using a phase modulator driven by a tunable RF synthesiser operating from 5 to 30 GHz. At high RF drive levels, the modulator generated higher-order sidebands in accordance with the Jacobi–Anger expansion, producing two optical combs centred on the seed laser frequencies. An optical band-pass filter with an approximate 10 GHz bandwidth was used to select overlapping spectral components, namely the positive-order upper sideband of the first laser and the corresponding lower-order sideband of the second laser. By jointly tuning the modulation frequency and the laser wavelengths, the selected third-order tones were maintained within 50 MHz of each other.

The filtered optical tones were detected using a 100 MHz-bandwidth photodiode followed by a transimpedance amplifier, generating an intermediate-frequency signal. This signal was compared with a 25 MHz reference in a phase–frequency detector to produce an error signal. Both the modulation source and the 25 MHz reference were phase-locked to a common 10 MHz reference oscillator to ensure system-wide coherence.

The resulting error signal was split and applied to two laser control units to enable frequency and phase locking. The frequency-lock loop (FLL) was implemented as a slow PI controller with a loop bandwidth of approximately 300 Hz, driving the piezo-based frequency tuning of one of the lasers. This loop compensates for frequency drifts and locks the inter-laser frequency difference to within 1 MHz. Once frequency locking was established, a fast loop was implemented to stabilise the relative optical phase between the two lasers, with an FM bandwidth of about 100 kHz. We estimate a loop delay of approximately 50 ns.

Noise Characterization

Noise and power measurements were carried-out using a cross-correlation based phase noise analyser (Rohde & Schwarz FSWP50), with a direct measurement for signal up to 50GHz. For >50GHz signal characterisation, band-specific frequency-conversion modules were employed: V-band (50-75 GHz), W-band (75-110 GHz), and D-band (110-170 GHz). The outputs from the photodiodes were split into two matched branches using a calibrated broadband power splitter, with each down converted to an IF. Both IF signals were simultaneously processed in the analyser's dual correlation channels, and cross-correlation averaging was applied to suppress the instrument noise floor in proportion to the square root of the number of averages. However, the D-band (110-170 GHz) signal power measurement of laser pair 2 signals were measured using a calibrated power meter due to the availability of the equipment, which might have led to the discrepancy shown in Fig.2a.

Frequency tunability

The frequency separation between the two lasers was established through a combination of coarse thermal tuning of the seed lasers and fine electronic tuning within the OHLL. Coarse thermal tuning enabled large adjustments of the beat frequency (on the order of hundreds of MHz) by varying the laser current and temperature set points. Fine tuning was achieved by adjusting the LO of the PFD, which is tunable from 0 to 40 MHz. This corresponds to an effective frequency offset tuning range from -25 MHz to +15 MHz relative to the 25 MHz centre frequency.

Fine control of the laser frequencies was implemented via precise adjustment of the frequency set points through the lasers' piezoelectric drivers. Following tuning, the IF signal remained phase-locked, and the long-term frequency accuracy was referenced to the common 10 MHz oscillator.

Millimetre-wave communication signal generation and processing

The communication signal is a 1-GBaud signal-carrier quadrature amplitude modulation (QAM) signal, pulse shaped by an RRC filter and digitally upconverted to 4.7 GHz centre frequency. The up-converted signal is generated using a 12-GSa/s arbitrary waveform generator (AWG) with 5-GHz analogue bandwidth and 10-bit digital resolution. The mixer upconverts the QAM signal to a double-side band (DSB) signal centred at 153 GHz and is subsequently filtered with a 135-150 GHz filter to create a single-side band (SSB) signal. At the receiver side, a state-of-the-art instrument synthesiser (Rohde & Schwarz SMA100B with ultra-low noise option) was employed as LO, which was multiplied to around 150 GHz to down convert the received signal to sub-10 GHz before being digitized by a 50 GSa/s ADC for DSP.

A variable RF attenuator is used to emulate link loss to study the receiver sensitivity. The digital signal generation and processing are implemented offline using MATLAB. The receiver DSP involves digital down-conversion, match filtering, clock and frame synchronization, and a digital equalizer [36]. Finally, the BER is calculated by processing the whole frame (20 µs for 16 QAM and 10 µs 64 QAM). The receiver sensitivity is characterised by measuring the BER and SNR at different received power.

5 Data availability

All data for the figures in this manuscript are available via UCL PRS.

6 Acknowledgements

The authors thank Rodhe & Schwarz for lending their phase noise characterization systems. Commercial equipment and trade names are identified for scientific clarity only, and doing so does not represent an endorsement by UCL. This research received support from EPSRC projects ORBITS (EP/V051377/1) and TRACCS (EP/W026252/1). Z. Liu acknowledges EPSRC Fellowship PROSPECT (EP/Z534444/1). A.K. acknowledges support from Department for Science, Innovation and Technology and the Royal Academy of Engineering Enterprise Fellowship.

7 Author Contributions

Z.L., A.K., A.B. and Z.Z. prepared the manuscript. Z.L. conceived the harmonic locking concept. A.K. and Z.L. developed and optimised the photonic frequency synthesiser approach. Z.Z., A.K. and Z.L. developed the mm-wave transmission system. A.K., A.B. and Z.Z. contributed to the phase noise and jitter characterizations. Z.Z., I.D. and Z. L. developed the mm-wave transmission experiments. Z.L. and Z.Z. developed and implemented the digital signal processing. All authors contributed to analysing the experimental results. Z.L. initiated and supervised the project.

8 Competing Interests Statement

A.K. and Z.L. are inventors on patent application No. PCT/EP2025/057707 related to the subject matter of this work. The other authors declare no competing interests.

9 Additional information

Correspondence and requests for materials should be addressed to Zhixin Liu. Supplementary information the online version contains supplementary material available at UCL RPS.

References

[1] Kudelin, I. *et al.* Photonic Chip-based Low-noise Microwave Oscillator. *Nature* **627**, 534–539 (2024).

[2] Kudelin, I. *et al.* An Optoelectronic Microwave Synthesizer with Frequency Tunability and Low Phase Noise. *Nature Electronics* **7**, 1170–1175 (2024).

[3] Tetsumoto, T. *et al.* Optically Referenced 300 GHz Millimetre-wave Oscillator. *Nature Photonics* **15**, 516–522 (2021).

[4] Spencer, D. T. *et al.* An Optical-frequency Synthesizer using Integrated Photonics. *Nature* **557**, 81–85 (2018).

[5] Palmann, C., Mavromatis, S., Hernández, M., Sequeira, J. & Brisco, B. Earth Observation using Radar Data: an Overview of Applications and Challenges. *International Journal of Digital Earth* **1**, 171–195 (2008).

[6] Kawanishi, T. *et al.* The Advanced Microwave Scanning Radiometer for the Earth Observing System (AMSR-E), NASDA's contribution to the EOS for global energy and water cycle studies. *IEEE Transactions on Geoscience and Remote Sensing* **41**, 184–194 (2003).

[7] Waters, J. W. *et al.* The Earth Observing System Microwave Limb Sounder (EOS MLS) on the Aura Satellite. *IEEE Transactions on Geoscience and Remote Sensing* **44**, 1075–1092 (2006).

[8] Schmalz, K. *et al.* Gas Spectroscopy System for Breath Analysis at mm-wave/THz Using SiGe BiCMOS Circuits. *IEEE Transactions on Microwave Theory and Techniques* **65**, 1807–1818 (2017).

[9] Zhou, Z., Kassem, A., Darwazeh, I. & Liu, Z. Ultra-low Phase Noise Photonic-generated Millimeter Wave to Overcome the Capacity Limitation in Electronic D-band (110-170 GHz) Signal Generation. In *2025 Optical Fiber Communications Conference and Exhibition (OFC)*, 1–3 (2025).

[10] Giordani, M. & Zorzi, M. Satellite Communication at millimeter waves: A key enabler of the 6G era. In *2020 International Conference on Computing, Networking and Communications (ICNC)*, 383–388 (IEEE, 2020).

[11] Santacruz, J. P., Rommel, S., Johannsen, U., Jurado-Navas, A. & Monroy, I. T. Analysis and Compensation of Phase Noise in mm-Wave OFDM ARoF Systems for Beyond 5G. *Journal of Lightwave Technology* **39**, 1602–1610 (2021).

[12] Poole, C. R. & Darwazeh, I. *Microwave Active Circuit Analysis and Design*, chap. 18 (Academic Press, Oxford, 2016), 2nd edn.

[13] Rubiola, E. *Phase Noise and Frequency Stability in Oscillators*. The Cambridge RF and Microwave Engineering Series (Cambridge University Press, 2008).

[14] Chen, J. *et al.* Influence of White LO Noise on Wideband Communication. *IEEE Transactions on Microwave Theory and Techniques* **66**, 3349–3359 (2018).

[15] Rohde & Schwarz. *R&S® SMA100B RF and Microwave Signal Generator, Specifications*. Rohde & Schwarz, Munich, Germany, version 09.00 edn. (2026). URL `https://scdn.rohde-schwarz.com/ur/pws/dl_downloads/pdm/cl_brochures_and_datasheets/specifications/5215_1018_22/SMA100B_specs_en_5215-1018-22_v0900.pdf`. Online.

[16] Matei, D. G. *et al.* 1.5 μm Lasers with Sub-10 mHz Linewidth. *Physical Review Letters* **118**, 263202 (2017).

[17] Fan, Y. *et al.* Hybrid Integrated InP-Si_3N_4 Diode Laser with a 40-Hz Intrinsic Linewidth. *Optics Express* **28**, 21713–21728 (2020).

[18] Xiang, C. *et al.* 3D Integration Enables Ultralow-noise Isolator-free Lasers in Silicon Photonics. *Nature* **620**, 78–85 (2023).

[19] Li, L. *et al.* Modified Uni-Travelling-Carrier Photodiodes with 206 GHz Bandwidth and 0.81 A W^{-1} External Responsivity. *Nature Photonics* **19**, 1301–1308 (2025).

[20] Beling, A., Bach, H.-G., Mekonnen, G. G., Kunkel, R. & Schmidt, D. High-Speed Miniaturized Photodiode and Parallel-Fed Traveling-Wave Photodetectors Based on InP. *IEEE Journal of Selected Topics in Quantum Electronics* **13**, 15–21 (2007).

[21] Runge, P. *et al.* Broadband 145GHz Photodetector Module Targeting 200GBaud Applications. In *2020 Optical Fiber Communications Conference and Exhibition (OFC)*, 1–3 (2020).

[22] Shin, D.-C., Kim, B. S., Jang, H., Kim, Y.-J. & Kim, S.-W. Photonic Comb-rooted Synthesis of Ultra-Stable Terahertz Frequencies. *Nature Communications* **14**, 790 (2023).

[23] Sun, S. *et al.* Microcavity Kerr Optical Frequency Division with Integrated SiN Photonics. *Nature Photonics* **19**, 637–642 (2025).

[24] Sun, S. *et al.* Integrated Optical Frequency Division for Microwave and mmWave Generation. *Nature* **627**, 540–545 (2024).

[25] Ji, Q.-X. *et al.* Dispersive-wave-agile Optical Frequency Division. *Nature Photonics* **19**, 624–629 (2025).

[26] Carpintero, G. *et al.* Microwave Photonic Integrated Circuits for Millimeter-Wave Wireless Communications. *Journal of Lightwave Technology* **32**, 3495–3501 (2014).

[27] Shen, X. *et al.* Compact Heterogeneously Integrated Optical Phase-Locked Loop for 10GHz to 40GHz Optical Frequency Difference Locking. *Journal of Lightwave Technology* **42**, 2784–2791 (2024).

[28] Torres-Company, V. & Weiner, A. M. Optical Frequency Comb Technology for Ultra-Broadband Radio-Frequency Photonics. *Laser & Photonics Reviews* **8**, 368–393.

[29] Kittlaus, E. A. *et al.* A Low-noise Photonic Heterodyne Synthesizer and its Application to Millimeter-wave Radar. *Nature Communications* **12**, 4397 (2021).

[30] IEEE Approved Draft Standard for Ethernet Amendment 2: Physical Layer Specifications and Management Parameters for 100 Gb/s Operation Over Backplanes and Copper Cables. *IEEE P802.3bj/D3.2, April 2014* 1–359 (2014).

[31] Liu, Z. & Slavík, R. Optical Injection Locking: From Principle to Applications. *Journal of Lightwave Technology* **38**, 43–59 (2020).

[32] Liu, Z., Farwell, S., Wale, M., Richardson, D. J. & Slavík, R. InP-based Optical Comb-Locked Tunable Transmitter. In *2016 Optical Fiber Communications Conference and Exhibition (OFC)*, 1–3 (2016).

[33] Kakarla, R., Schröder, J. & Andrekson, P. A. Optical Injection Locking at Sub-nano-watt Powers. *Optics Letters* **43**, 5769–5772 (2018).

[34] Franken, C. A. A. *et al.* High-power and Narrow-Linewidth Laser on Thin-Film Lithium Niobate enabled by Photonic Wire Bonding. *APL Photonics* **10**, 026107 (2025).

[35] Balakier, K., Ponnampalam, L., Fice, M. J., Renaud, C. C. & Seeds, A. J. Integrated Semiconductor Laser Optical Phase Lock Loops. *IEEE Journal of Selected Topics in Quantum Electronics* **24**, 1–12 (2018).

[36] Zhou, Z. *et al.* Communications with Guaranteed Bandwidth and Low Latency using Frequency-Referenced Multiplexing. *Nature Electronics* **6**, 694–702 (2023).

Supplementary Files

This is a list of supplementary files associated with this preprint. Click to download.

- supplementary.pdf